

Cite this: *Digital Discovery*, 2023, 2,
409

SolvBERT for solvation free energy and solubility prediction: a demonstration of an NLP model for predicting the properties of molecular complexes†

Jiahui Yu,^a Chengwei Zhang,^b Yingying Cheng,^b Yun-Fang Yang,^b
Yuan-Bin She,^b Fengfan Liu,^a Weike Su^a and An Su^{*b}

Deep learning models based on NLP, mainly the Transformer family, have been successfully applied to solve many chemistry-related problems, but their applications are mostly limited to chemical reactions. Meanwhile, solvation is an important concept in physical and organic chemistry, describing the interaction of solutes and solvents. In this study, we introduced the SolvBERT model, which reads the solute and solvent through the SMILES representation of their combination. SolvBERT was pre-trained in an unsupervised learning fashion using a large database of computational solvation free energies. The pre-trained model could be used to predict the experimental solvation free energy or solubility, depending on the fine-tuning database. To the best of our knowledge, this multi-task prediction capability has not been observed in previously developed graph-based models for predicting the properties of molecular complexes. Furthermore, the performance of our SolvBERT in predicting solvation free energy was comparable to the state-of-the-art graph-based model DMPNN, mainly due to the clustering feature of the pre-training phase of the model, as demonstrated using the TMAP visualization algorithm. Last but not least, our SolvBERT outperformed the recently-developed GNN-Transformer hybrid model, GROVER, in predicting a set of experimentally evaluated solubility data with out-of-sample solute-solvent combinations.

Received 6th October 2022
Accepted 29th January 2023

DOI: 10.1039/d2dd00107a

rsc.li/digitaldiscovery

Introduction

The use of deep learning models to study the chemical sciences is rapidly increasing, especially in subfields including synthetic planning^{1,2} and automatic chemical designing.^{3,4} From a model architecture perspective, the two most commonly used deep learning architectures for chemistry-related problems are graph-based models and text-based natural language processing (NLP) models. Graph-based models, including graph convolutional networks (GCN),^{5,6} message passing neural networks (MPNN),⁷ and the recently developed directed-MPNN (D-MPNN),⁸ have mostly been applied to the prediction of molecular properties.^{9–13} On the other hand, NLP models, mainly the Transformer¹⁴ family, have been mainly applied to the study of chemical reactions, such as the prediction of forward reaction outcomes^{15–17} and retrosynthetic pathways^{18–20} as well as

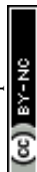
inferring reaction mechanisms^{21–23} and experimental procedures.^{24,25} Previously, the application of NLP models in chemistry was mostly limited to chemical reactions, one reason being that early NLP models were sequence-to-sequence – the models could only read in and output text-based representations. However, due to the rapid development of the Transformer family, a model called Bidirectional Encoder Representations from Transformers (BERT)²⁶ was built for classification and regression tasks. Two recent studies by Schwaller *et al.* used BERT to predict the classifications²⁷ and yields²⁸ of chemical reactions, demonstrating the potential of NLP models for predicting numerical properties.

In addition to reactions, solvation is another type of molecular interaction that describes the interaction of a solvent with a dissolved molecule, in which the solute and solvent reorganize into a solvation complex.^{29,30} Solvation free energy and solubility are two physical properties commonly used to describe solvation.^{31,32} Solvation free energy is the change in free energy associated with the transfer of a molecule between the ideal gas and a solvent at a given temperature and pressure.³³ Solubility is a parameter used to assess how much of a substance can remain in solution without precipitating and is defined as the maximum amount of a solute that can dissolve in a solvent under given physical conditions (pressure, temperature, pH, etc.).³⁴ The prediction of these solvation properties can facilitate

^aNational Engineering Research Center for Process Development of Active Pharmaceutical Ingredients, Collaborative Innovation Center of Yangtze River Delta Region Green Pharmaceuticals, Zhejiang University of Technology, Hangzhou, 310014, PR China

^bCollege of Chemical Engineering, Zhejiang University of Technology, Hangzhou, 310014, PR China. E-mail: ansu@zjut.edu.cn

† Electronic supplementary information (ESI) available. See DOI: <https://doi.org/10.1039/d2dd00107a>



solvent screening in drug design, synthesis route design, process intensification, and crystallization.^{31,35}

Using machine learning and deep learning to predict the relevant properties of solvation can save the expensive time and cost of performing experiments or computations, and also help to find important features that contribute to the solvation properties.³⁶ Recent studies by Vermeire *et al.* and Zhang *et al.* both pre-trained graph-based neural networks on computational solvation free energy datasets and then used smaller experimental solvation free energy datasets for transfer learning. A potential drawback of using supervised learning in the pre-training phase is that it may lead to negative transfer (*i.e.*, result in undesirable degradation of model performance) when transferring knowledge from pre-training on one attribute (*e.g.*, solvation free energy) to the prediction of another attribute (*e.g.*, solubility).^{37–39} In contrast, BERT, a new generation of NLP models, does not have this drawback because its pre-training phase is completely unsupervised (does not depend on data labels). Furthermore, to our knowledge, few NLP-based models have been used to study solvation.^{40,41} Given the success of the above NLP models in predicting chemical reactions, it is likely that NLP models can also study different types of molecular interactions, such as solvation.

Therefore, in this study, we introduced a BERT-based regression model, SolvBERT, to predict two properties of solvation, namely solvation free energy and solubility. Instead of inputting the solute and solvent separately, SolvBERT reads the SMILES of solute–solvent combinations and converts the SMILES combination into vectorized representations. We trained SolvBERT using three different databases computed or curated in previous studies.^{42,43} We also compared this model with state-of-the-art graph-based models, one graph-input NLP model, and a traditional machine learning model to further discuss the impact of model architecture in predicting the properties of molecular complexes. Also, TMAP, an advanced tree-based algorithm for visualizing high-dimensional data, was used to show the benefits of SolvBERT in clustering solvent–solute combinations. Finally, we measured the solubility of 21 solute–solvent combinations as out-of-sample data to experimentally evaluate the performance of SolvBERT.

Methods

Datasets

CombiSolv-QM. The CombiSolv-QM dataset, which originally came from a study by Vermeire *et al.*, was used as a pre-

training dataset in our study without any modification. The dataset consists of 1 million datapoints randomly selected from all possible combinations of 284 commonly used solvents and 11 029 solutes. A detailed description can be retrieved from ref. 44.

CombiSolv-Exp-8780. The CombiSolv-Exp dataset originally contained experimental solvent free energy data for 10 145 different solute and solvent combinations from Vermeire *et al.*⁴⁴ The dataset was curated from multiple sources, including the Minnesota solvation database,⁴⁵ the FreeSolv database,⁴⁶ the CompSol database,⁴⁷ and a dataset published by Abraham *et al.*⁴⁸ Unfortunately, to the best of our knowledge, only 8780 of these 10 145 data instances are publicly available. Therefore, we downloaded data from these 8780 instances and renamed this dataset as CombiSolv-Exp-8780 to distinguish it from the original CombiSolv-Exp dataset. We compared the distribution of solvation free energy for our CombiSolv-Exp-8780 and the original CombiSolv-Exp in Vermeire *et al.*'s study⁴⁴ and found no significant differences in their distributions (Fig. S1 in the ESI†).

Solubility. The solubility dataset was originally from Boobier *et al.*⁴³ It was curated from the open notebook science challenges water solubility dataset and the Reaxys database. This dataset includes ethanol with 695 solutes, benzene with 464 solutes, acetone with 452 solutes, and water with 900 solutes, for a total of 2511 different combinations, with solubility expressed as $\log S$.

SMILES representation. Each SMILES of the solute–solvent combination in the three datasets was represented in the format of <SMILES of solvent>.<SMILES of solute> (Fig. 1). For example, as shown in Fig. 1a, water as a solvent containing 1,1,1,2,2-pentafluoro-2-(trifluoromethoxy)ethane as a solute was shown as “O.FC(F)(F)OC(F)(F)C(F)(F)F”.

Model names and architectures

SolvBERT. We built our SolvBERT on the open-source model architecture rxnfp (<https://rxn4chemistry.github.io/rxnfp/>), which was originally built for chemical reaction classification,²⁷ and made a few changes to adapt it for predicting solvation properties. The first change was on the tokenizer. In NLP models, a tokenizer is used to encode words and sentences and extract their linguistic features. In this study, we need the tokenizer to convert the SMILES of solute–solvent combinations into a machine understandable markup language. Since the tokenizer of rxnfp was originally designed

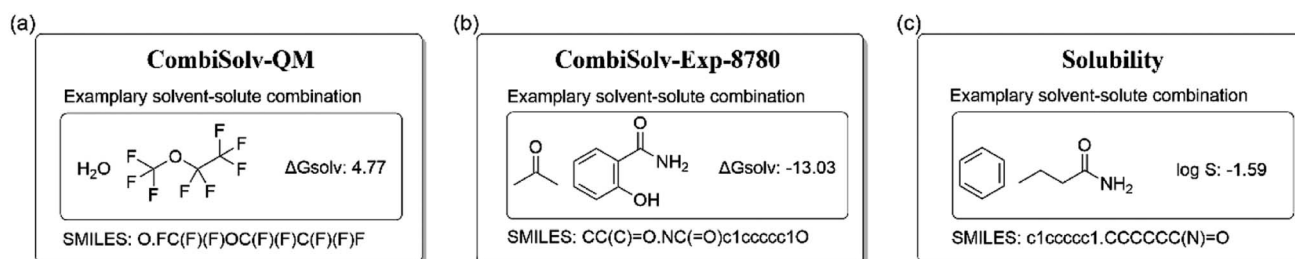


Fig. 1 SMILES representation of solvent–solute combinations.



Index	Token	...	26	C	...	4302	C2CC1CCCC1CC2
1	[UNK]		27	F		4303	C3CCC1
2	[CLS]		28	H		4304	OCC1CC1CC
3	[SEP]		29	I		4305	C1CCCOC1

Fig. 2 Vocabulary created by using tokenizer based on the combine-QM database.

for chemical reactions, we replaced it with the tokenizer from the hugging face framework (https://huggingface.co/docs/transformers/main_classes/tokenizer). The tokenizer uses byte pair encoding (BPE) to build vocabulary for the model (Fig. 2)

Similar to other BERT models for chemistry-related problems,^{27,49} SolvBERT performs a masked language model (MLM) learning task in the pre-training phase. MLM is a fill-in-the-blank task in which the model predicts the masked words based on the contextual words surrounding the mask tokens.⁵⁰ SolvBERT was pre-trained by performing the MLM task of the SMILES combinations from CombiSolv-QM, where individual atoms of the input SMILES were masked with a probability of 0.15. In addition, a special class token [CLS] was prepended to the tokenized SMILES but was never masked during this pre-training phase. In contrast to the original rxnfp that uses the [CLS] as a classification header for reaction classification, SolvBERT uses the [CLS]-labeled embedding as the input for the regression head for predicting solvation-related properties. Furthermore, based on the default parameters of the original rxnfp framework, the hyperparameters of SolvBERT were further optimized, including batch size, learning rate, hidden dropout rate, and the number of training epochs.

GCN. Graphical convolution networks (GCN) read molecules as graphs – which represent atoms and bonds with vertices and edges, respectively – and then combine the graphical descriptors on the convolutional layers. We used the model from DeepChem (https://deepchem.readthedocs.io/en/2.6.1/api_reference/models.html#graphconvmodel) which was implemented based on the work of Duvenaud *et al.*⁵ As with SolvBERT, we trained the GCN in two ways. (1) GCN-QM-Exp: pre-training with CombiSolv-QM and finetuning with CombiSolv-Exp-8780 and (2) GCN-Exp: single training with

CombiSolv-Exp-8780 (Table 1). The hyperparameters were optimized using the Gaussian process hyperparameter optimization algorithm provided by DeepChem.

D-MPNN. Directed-message passing neural network (D-MPNN)⁸ reads both graphical representation of molecules like GCN and molecular descriptors and fingerprints, and has been reported to outperform the models based on either graphical neural architectures or molecular fingerprints and descriptors.⁵¹ We used the D-MPNN implementation of Yang *et al.* (<https://github.com/chemprop/chemprop>) and trained the model in a similar manner to GCN (Table 1).

MinHash fingerprint (MHFP). As traditional ML models usually take molecular descriptors or fingerprints as description of molecular structures, we used MHFP6 (MinHash fingerprint, up to six bonds)⁵² to extract molecular fingerprints. MHFP6 is a molecular fingerprint that extracts SMILES of all circular substructures around each atom with no more than 6 bonds in diameter and applies the MinHash method to the resulting set, enabling the local sensitive hash (LSH) approximate to facilitate the performance of nearest neighbor search.

Random forest (RF). A traditional machine learning (ML) model, random forest (RF), was included as one of the baseline models. Two hyperparameters of the RF, the number of estimators and the maximum depth, were optimized through grid search and cross validation.

GROVER. GROVER is a recently developed hybrid GNN-Transformer model with the full name of “Graph Representation from self-supervised message passing transformer”, which feeds the graph representation of molecules into Transformer.³⁹ In more detail, GROVER consists of a node GNN Transformer and an edge GNN Transformer, which are similar in structure, differing only in the features processed. One of the

Table 1 Name and architecture of the models and the datasets for training

Model architecture	Molecular representation	Model name	Dataset for pre-training	Dataset for fine-tuning
SolvBERT	SMILES	SolvBERT-QM-Exp	CombiSolv-QM	CombiSolv-Exp-8780
		SolvBERT-Exp	CombiSolv-Exp-8780	
		SolvBERT-QM	CombiSolv-QM	
		SolvBERT-QM-logS	CombiSolv-QM	Solubility
		SolvBERT-logS	Solubility	
GCN	Graphs	GCN-QM-Exp	CombiSolv-QM	CombiSolv-Exp-8780
		GCN-Exp	CombiSolv-Exp-8780	
		D-MPNN-QM-Exp	CombiSolv-QM	CombiSolv-Exp-8780
D-MPNN	Graphs	D-MPNN-Exp	CombiSolv-Exp-8780	
		GROVER-Exp	CombiSolv-Exp-8780	
GROVER	Graphs	GROVER-logS	Solubility	
		RF-Exp	CombiSolv-Exp-8780	



GNN modules is specifically designed to transform the information of the graph into the features required by the Transformer. Similar to other sequence-based models, GROVER uses transfer learning to improve the training efficiency and accuracy of downstream tasks. In the pre-training phase, the model is designed with contextual property prediction and graph-level motif prediction. It should be emphasized that, similar to our SolvBERT, the pre-training process does not require supervised labeling (*i.e.*, only the molecular SMILES are required), which not only avoids negative impact on the downstream tasks, but also greatly reduces the difficulty of data acquisition. In our work, we fine-tuned the pre-trained model GROVER-base³⁹ directly with the CombiSolv-Exp-8780 dataset, where GROVER-base was initially trained on 11 million unlabeled molecules from the ZINC15 (ref. 53) and ChEMBL⁵⁴ datasets.

TMAP. TMAP⁵⁵ is a dimensionality reduction algorithm capable of handling millions of data points. The advantage of TMAP over other dimensionality reduction algorithms is that its output is a two-dimensional tree structure. The tree-based layout preserves global and local features by explicitly visualizing the detailed structure of branches and sub-branches, and enables high-resolution visualization of the structural features of the molecule. The algorithm consists of four steps: (1) forest-based LSH index,⁵⁶ (2) construction of *c*-approximate *k*-nearest neighbor graph, (3) calculation of a minimum spanning tree (MST) of the *c*-approximate *k*-nearest neighbor graph,⁵⁷ and (4) generation of a layout for the resulting MST. The generated layout is then displayed using faerun, an interactive data visualization framework.⁵⁸ Notably, the Kruskal algorithm is used at the stage of generating the minimum spanning tree to select the local optimal solution at each stage to obtain the global optimal solution and remove all the cycles in the initial graph. This significantly reduces the computational complexity of the low-

dimensional embedding and enhances the capture of the local structure of the data.

Evaluation metrics. The coefficient of determination (R^2), root mean square error (RMSE), and mean absolute error (MAE) were chosen to evaluate the performance of models. They are calculated as follows:

$$R^2 = 1 - \frac{\sum_{i=1}^m (y_i - \hat{y}_i)^2}{\sum_{i=1}^m (y_i - \bar{y})^2}$$

$$\text{RMSE} = \sqrt{\frac{1}{m} \sum_{i=1}^m (y_i - \hat{y}_i)^2}$$

$$\text{MAE} = \frac{1}{m} \sum_{i=1}^m |y_i - \hat{y}_i|$$

Results

Training SolvBERT

To fully evaluate the performance of the SolvBERT model without the potential interference of data scarcity, we first pre-trained and fine-tuned the model using the CombiSolv-QM dataset, which contained the computed solvation free energy of ~ 1 million solute-solvent pairs (Fig. 3, left part). In the pre-training phase, the model was trained with SMILES of solute-solvent combinations without any property data. Fig. S2† in the ESI† provides learning curves showing the losses of the training and validation sets in relation to the training steps. The losses in both the training and evaluation set decreased sharply in 1000 steps and then gradually decreased to a stable minimum

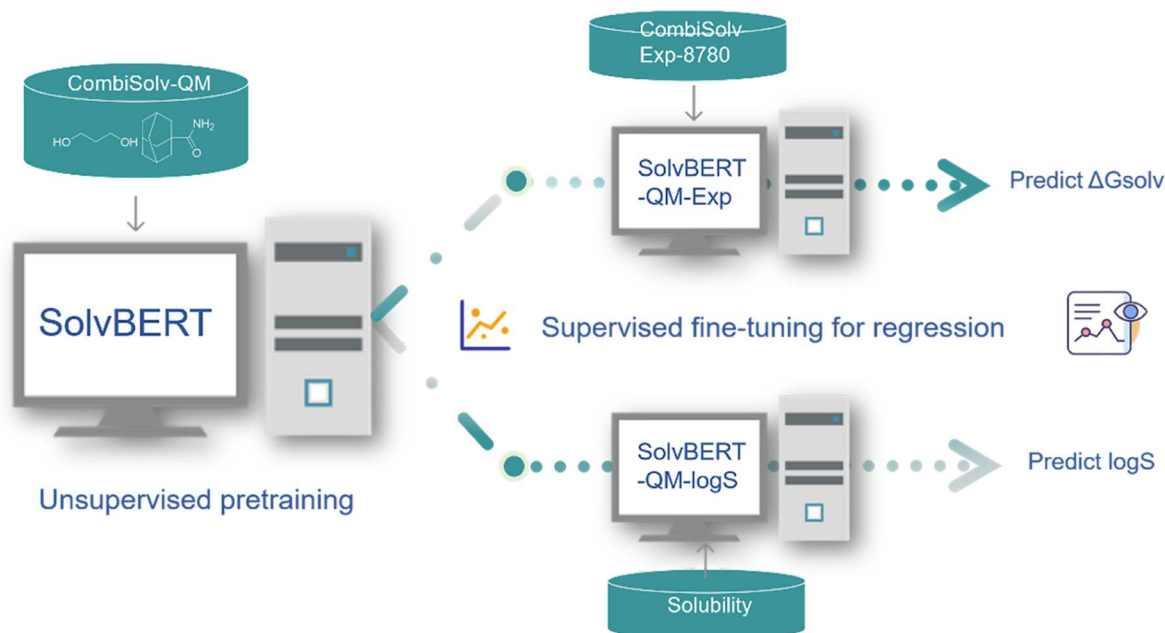


Fig. 3 Workflow of SolvBERT, including pre-training, finetuning, and property prediction.



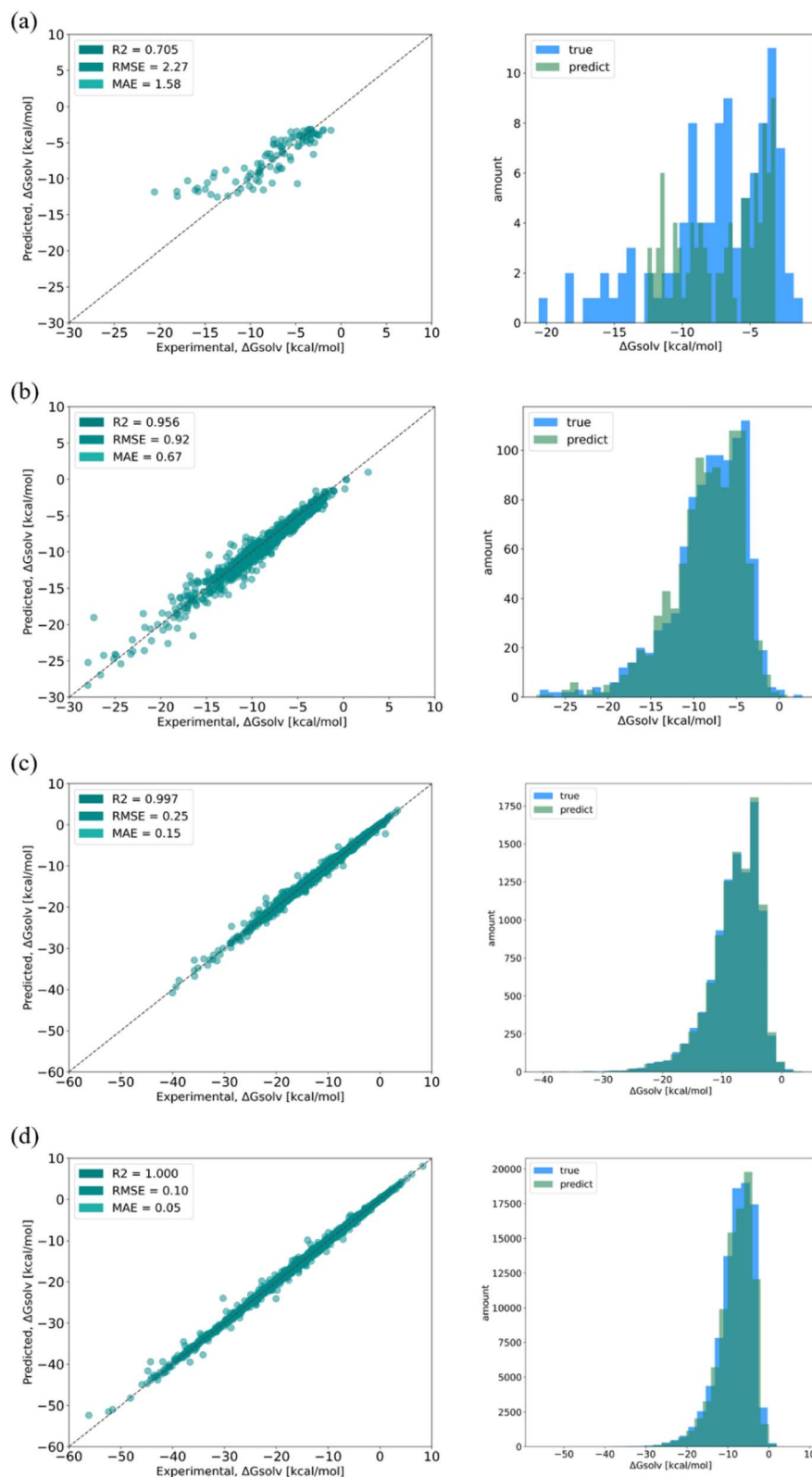


Fig. 4 Regressions (left column) and distributions (right column) of true and predicted values of solvation free energy from the SolvBERT model trained on the CombiSolv-QM dataset of different sizes: (a) 10^3 , (b) 10^4 , (c) 10^5 , and (d) 10^6 .

by 8000 steps. No overfitting is observed since the validation loss does not show a significant increase with decreasing training loss.⁵⁹ Afterward, the same solute–solvent complexes

were provided along with the corresponding free energy data for the fine-tuning stage. The final RMSE/MAE for test sets are shown in Fig. 4d (where the dataset size is 10^6).



Table 2 Performance of SolvBERT-QM-Exp and SolvBERT-Exp on the training and validation of the CombiSolv-Exp-8780 dataset

Model	Training			Validation		
	R^2	RMSE (kcal mol ⁻¹)	MAE (kcal mol ⁻¹)	R^2	RMSE (kcal mol ⁻¹)	MAE (kcal mol ⁻¹)
SolvBERT-QM-Exp	0.990	0.45	0.30	0.981	0.60	0.37
SolvBERT-Exp	0.984	0.58	0.38	0.964	0.83	0.51

In addition, the effect of the size of the training dataset was evaluated by using different proportions of the CombiSolv-QM dataset (Fig. 4). Considering that the mean value of the solvation free energy in the dataset is -8.10 kcal mol⁻¹, the size of the training dataset needs to be more than 10^5 to reach a relative error of less than 10% when using the same dataset in the pre-training and fine-tuning phases. The effect of training set size was also assessed using the distribution of predicted values and true values (Fig. 4, right column). As the training sizes increased, the overlap of the distributions became more pronounced, with significant overlap observed when the size does not fall below 10^5 (Fig. 4c and d).

Transfer learning of solvation free energy and solubility. Transfer learning can help deep learning models learn from larger and cheaper datasets (*e.g.*, high-throughput computational data) and apply the learned knowledge to further training on smaller and more expensive datasets (*e.g.*, experimental data). Here, we present the benefits of transfer learning on two datasets, CombiSolv-Exp-8780, a subset of a solvation free energy dataset acquired experimentally, and solubility, a dataset curated by Boobier *et al.* that describes the solvation in terms of solubility rather than solvation free energy.

SolvBERT-QM-Exp is a SolvBERT model pre-trained on the CombiSolv-QM dataset and fine-tuned on the CombiSolv-Exp-

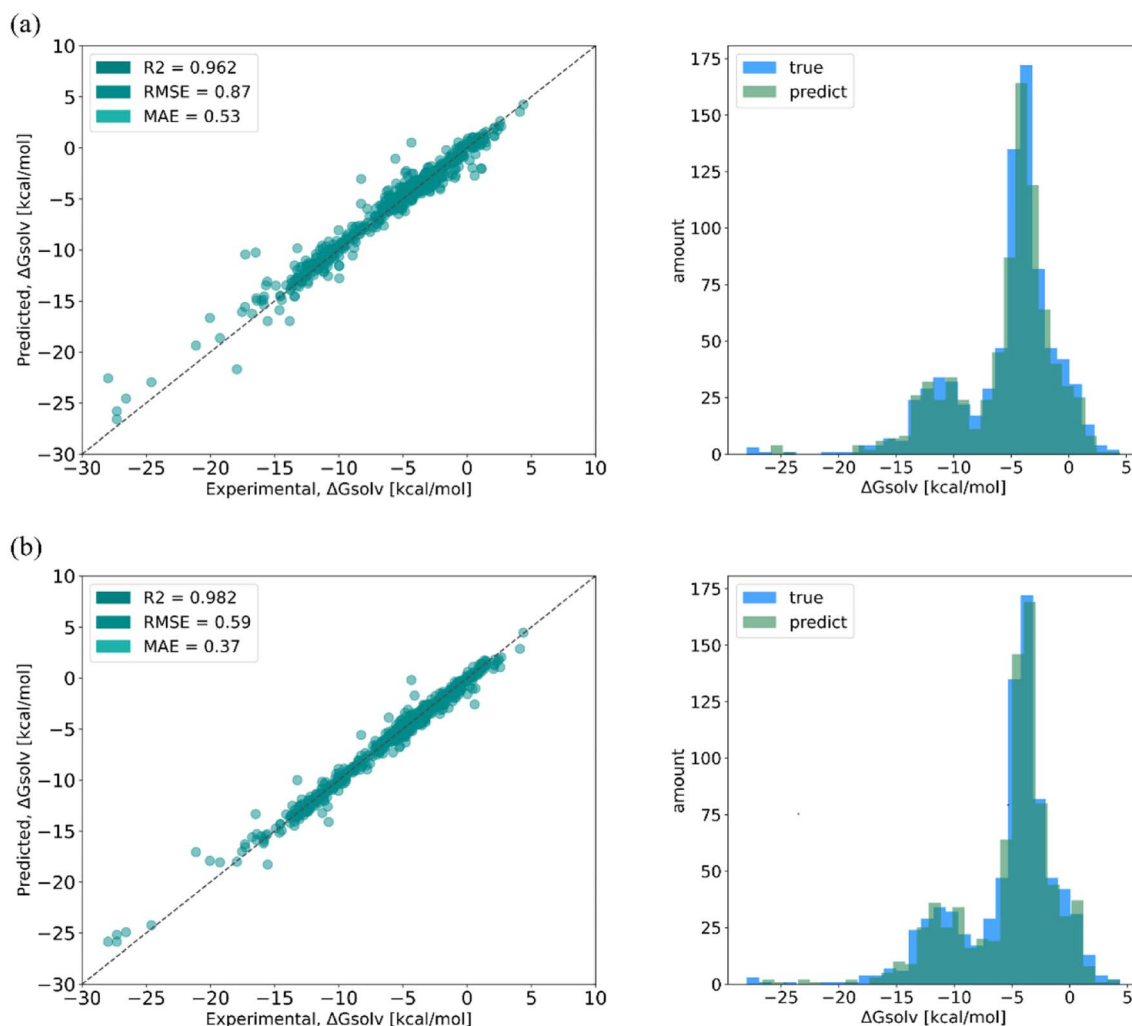


Fig. 5 Regressions (left column) and distributions (right column) of true and predicted values of solvation free energy from (a) SolvBERT-QM-Exp and (b) SolvBERT-Exp.



8780 dataset (Fig. 3, upper right). After optimization, hyperparameters including an epoch of 20, a batch size of 16, a learning rate of 0.00008 and a hidden dropout rate of 0.4 were selected (Table S4 in the ESI†). To demonstrate the benefits of pre-training with CombiSolv-QM, we pre-trained and fine-tuned another SolvBERT model using only the CombiSolv-Exp-8780 dataset, resulting in the SolvBERT-Exp model for comparison. It was found that SolvBERT-QM-Exp outperformed SolvBERT-Exp – SolvBERT-QM-Exp had a higher R^2 and lower RMSE and MAE in both training and validation results (Table 2). For the test set, the distributions of predicted and true values of SolvBERT-QM-Exp overlapped slightly more than those of SolvBERT-Exp, while the regression plot diverges less (Fig. 5).

Previous studies have found that the benefits of pre-training on large datasets are more pronounced when the size of the fine-tuning dataset is small. To see if this phenomenon existed in our case, we extracted different proportions from the CombiSolv-Exp-8780 dataset for fine-tuning the SolvBERT-QM-Exp model and training and fine-tuning the SolvBERT-Exp model. The results show that the prediction error of SolvBERT-Exp is significantly higher than that of SolvBERT-QM-Exp when the size of CombiSolv-Exp-8780 is less than 20% of its original size, which indicates that pre-training the model using CombiSolv-QM has a more obvious advantage when the size of the fine-tuning dataset is small (Fig. 6).

Since the pre-training stage of SolvBERT was unsupervised, which means the pre-training does not require any property data, it is possible to pre-train the model using the data from property A (e.g., the CombiSolv-QM dataset, size = 1 million) and fine-tune using the data from property B (e.g., the solubility

dataset, size = 2511), as long as both properties are for the same target (e.g., solvation), which is important when the data size of property B is significantly smaller than that of property A. Here, we proposed two additional combinations of models and datasets – SolvBERT-logS using the solubility dataset for pre-training and fine-tuning, and SolvBERT-QM-logS using the CombiSolv-QM dataset for pre-training and the solubility dataset for fine-tuning (Fig. 2, lower right). Since the solubility dataset was significantly smaller than the CombiSolv-Exp-8780 dataset, we increased the epochs to 60, while keeping the other hyperparameters the same as in the SolvBERT-QM-Exp model. The results show that the solubility prediction performance of the model is significantly improved with lower RMSE and MAE and higher R^2 by pre-training with the CombiSolv-QM dataset (Table 3).

Comparing SolvBERT with benchmark models. There are two main approaches to transfer learning, namely fine-tuning and feature-based. BERT uses a fine-tuning approach, in which all parameters are being fine-tuned during the training process of supervised learning, instead of a feature-based approach where the features learned in the pre-training phase are fixed in transfer learning.²⁶ Unlike Vermeire *et al.*⁴⁴ who performed feature-based transfer learning on D-MPNN, we performed fine-tuning transfer learning on both GCN and D-MPNN in order to compare them with BERT in a fair manner. The two graph-based models were pre-trained with the CombiSolv-QM dataset and fine-tuned with the CombiSolv-Exp-8780 dataset. Models trained directly on the CombiSolv-Exp-8780 dataset were also included (Table 4). The results show that our SolvBERT-QM-Exp model performs comparably to the

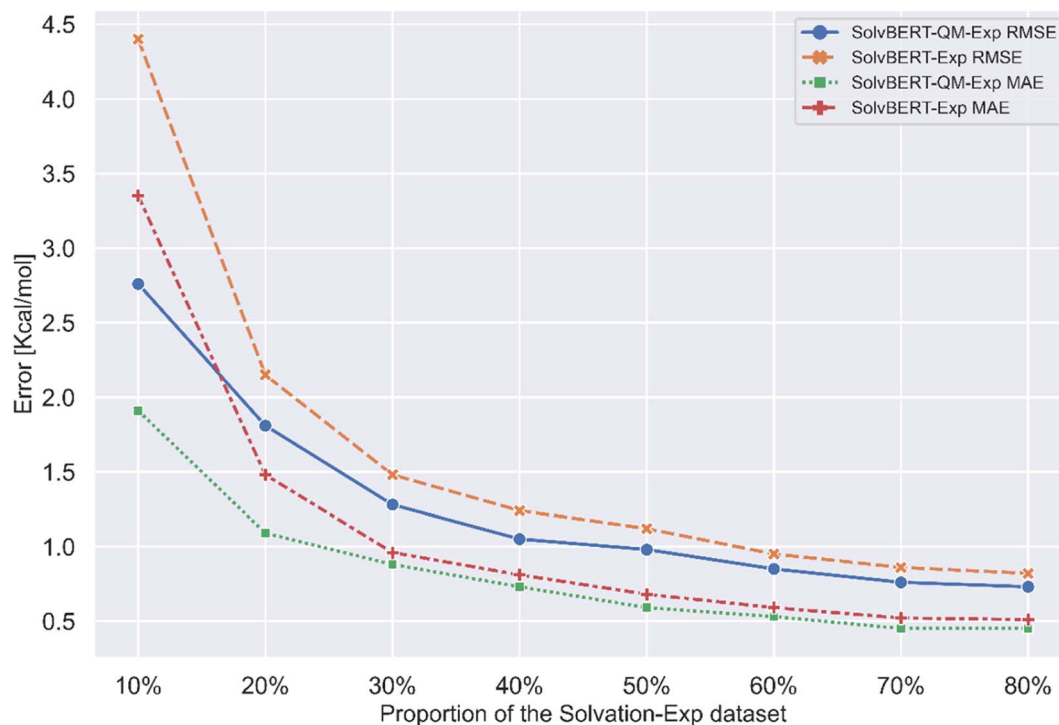


Fig. 6 Performance of the SolvBERT-QM-Exp and SolvBERT-Exp models fine-tuned with different proportions of the CombiSolv-Exp-8780 dataset.



Table 3 Performance of SolvBERT models and GROVER on the training, validation, and test sets of the solubility dataset. SolvBERT-logS refers to the SolvBERT model directly trained on the solubility dataset without pre-training, while SolvBERT-QM-logS stands for the SolvBERT model pre-trained with CombiSolv-QM before fine-tuning with the solubility dataset. GROVER came with its default pre-trained parameters and was fine-tuned with the solubility dataset

Model	Training			Validation			Test		
	R^2	RMSE	MAE	R^2	RMSE	MAE	R^2	RMSE	MAE
SolvBERT-logS	0.870	0.69	0.54	0.65	1.08	0.82	0.73	1.10	0.86
SolvBERT-QM-logS	0.921	0.54	0.38	0.926	0.52	0.38	0.925	0.47	0.36
GROVER-logS	0.903	0.60	0.43	0.908	0.59	0.44	0.935	0.49	0.38

Table 4 Performance of different benchmark models on the training, validation, and test sets of the CombiSolv-Exp-8780 dataset. The units for RMSE and MAE are kcal mol⁻¹

Model	Training			Validation			Test		
	R^2	RMSE	MAE	R^2	RMSE	MAE	R^2	RMSE	MAE
GCN-Exp	0.896	1.36	1.01	0.893	1.50	1.04	0.905	1.36	0.97
GCN-QM-Exp	0.906	1.4	0.88	0.926	1.24	0.91	0.929	1.18	0.88
DMPNN-Exp ^a	0.901	1.44	0.96	0.894	1.47	1.00	0.885	1.55	1.07
DMPNN-QM-Exp ^a	0.989	0.48	0.29	0.988	0.51	0.32	0.974	0.73	0.43
GROVER-Exp	0.982	0.61	0.37	0.984	0.61	0.37	0.979	0.64	0.38
RF-Exp	0.636	2.26	1.56	0.742	1.79	1.36	0.694	1.95	1.40

^a The transfer learning of the DMPNN model is by a fine-tuning approach rather than by a feature-based approach. Both the method and the results of transfer learning differ from those of the study by Vermeire *et al.*⁴⁴

DMPNN-QM-Exp model – DMPNN performs slightly better on the validation set (R^2 0.007 higher, RMSE 0.09 lower, and MAE 0.05 lower), while SolvBERT performs better on the test set (R^2 0.008 higher, RMSE 0.14 lower, and MAE 0.06 lower). Furthermore, our SolvBERT-QM-Exp model performs comparably to the graph-input NLP model: GROVER-Exp performs slightly better on the validation set with R^2 being 0.003 higher, RMSE being 0.01 higher, and MAE being the same, while SolvBERT performs better on the test set with R^2 being 0.003 higher, RMSE being 0.05 lower, and MAE being 0.01 lower. Considering that both DMPNN and GROVER have been reported as state-of-the-art models for predicting molecular properties,⁵¹ the performance of our SolvBERT was satisfactory.

Mapping the chemical space of solvation. Small molecules described using MHFP have been used by TMAP⁵⁵ to visualize the chemical space of small-molecule databases such as ChEMBL, Drugbank, and DSSTox (<https://tmap.gdb.tools/>, accessed on Dec. 23, 2022). In this study, we visualized the chemical space of the CombiSolv-Exp-8780 dataset, where solute–solvent combinations are represented in two ways: MHFP (Fig. 7, left) and the vector representation of SolvBERT-extracted fingerprints (*i.e.* SolvBERT-fp). SolvBERT-fp extracted after the pre-training phase (*i.e.* SolvBERT-fp-pre-trained, Fig. 7, lower right) and after the finetuning phase (*i.e.* SolvBERT-fp-finetuned, Fig. 7, upper right) are shown, respectively.

While the solute–solvent combinations described by MHFP do not show a clear relationship between clustering and solvation free energy (Fig. 7, left) those described by SolvBERT-fp-pre-trained show a significantly improved clustering of solute–solvent combinations. Clustering is broadly divided into four

regions, red (0–5 kcal mol⁻¹), red-orange (–10 to 0 kcal mol⁻¹), green-blue (–20 to –10 kcal mol⁻¹), and blue-purple (–20 to –30 kcal mol⁻¹). Obviously, the vectorized representation of the pre-training phase output using SolvBERT, has a better association between clustering on TMAP and the free energy, although we did not train with the solvation free energy data in the pre-training phase.

The SolvBERT-fp-finetuned shows an even better clustering closely related to the value of solvation free energy. We can see the exemplary solvent–solute combination in the solid line box at the bottom left of Fig. 7, in which the solute is 9-hydroxy-5-(3,4,5-trimethoxyphenyl)-5,8,8a,9-tetrahydrofuro[3',4':6,7]naphtho[2,3-d][1,3]dioxol-6(5aH)-one and the solvent is propan-2-ol, with the solvation free energy being –25.12 kcal mol⁻¹. This combination, represented by blue color, is trapped in a green cluster in the MHFP chemical space (Fig. 7, upper left). In contrast, the combination is located in a clearly demonstrated blue cluster in both SolvBERT-fp-pre-trained and SolvBERT-fp-finetuned.

Out-of-sample test through experimental evaluation. To evaluate the ability of the SolvBERT model to predict the properties of solvent–solute combination with solvents and/or solutes that did not appear in the training progress, we performed experiments to measure the solubility of the following three combinations: (a) only the solute was out-of-sample (*i.e.*, not present in the solubility training set) (Table 5); (b) only the solvent was out-of-sample (Table 6); (c) both the solute and the solvent were out-of-sample (Table 7). The procedures for solubility measurement are provided in the ESI.† The predictions of



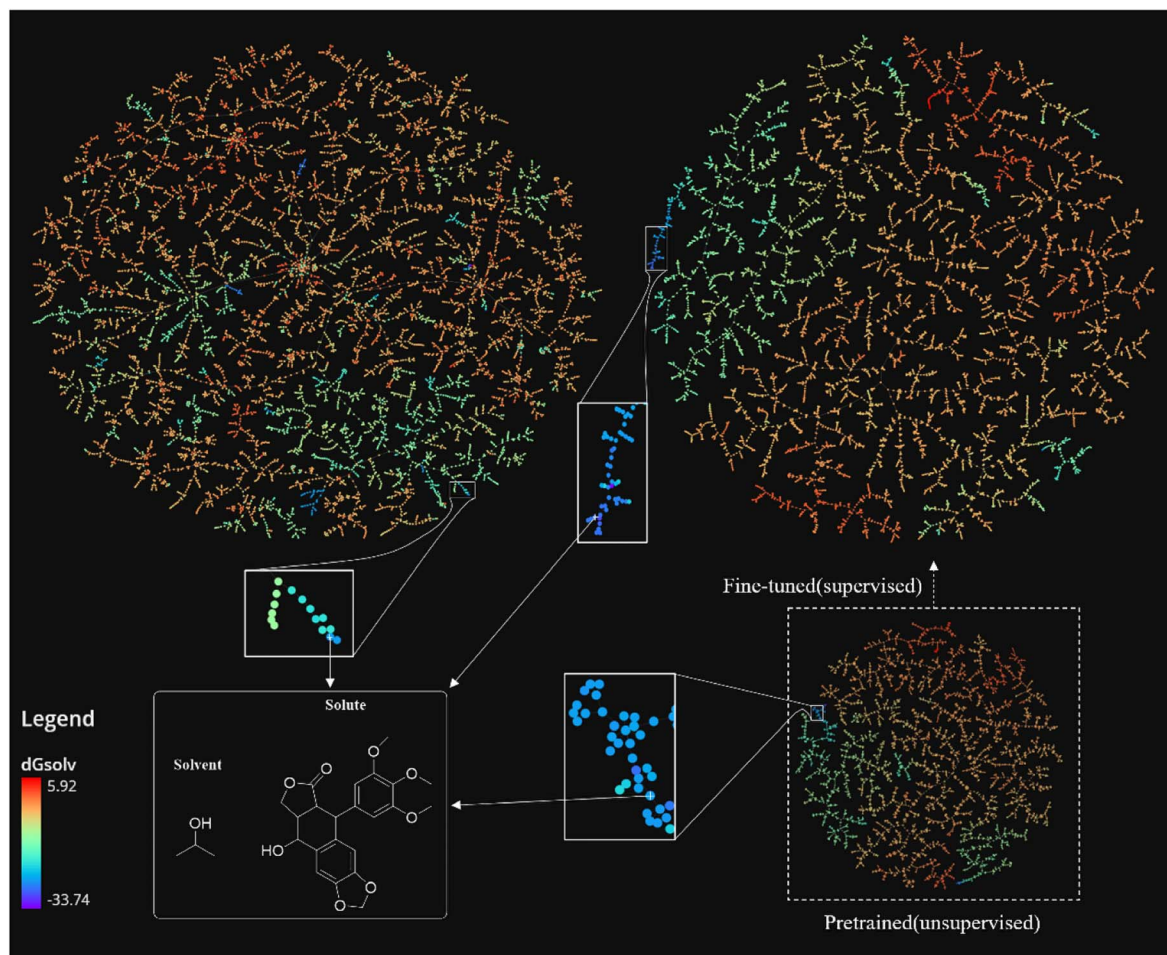


Fig. 7 TMAP visualization of the CombiSolv-Exp-8780 dataset based on three different types of fingerprints: the MHPF fingerprint on the upper left without SolvBERT processing, the fingerprint generated by the fine-tuning model based on SolvBERT (SolvBERT-fp-finetuned) on the upper right, and the dashed box on the lower right shows the fingerprints generated by the unsupervised learning model during the pre-training process (SolvBERT-fp-pre-trained). The color bars are from high (red) to low (blue) depending on the value of solvation free energy.

Table 5 Experimentally measured, SolvBERT-predicted, and GROVER-predicted solubility (g/100 g) with out-of-sample solutes and in-sample solvents. Experiments were performed at room temperature and 101.325 kPa

In-sample solvent		Out-of-sample solute		
		O-Methyl-N-nitroisourea	3-Methyl-2-nitrobenzoic acid	2-Amino-5-chloro-3-methylbenzoic acid
Acetone	Measured	2.5148	4.8715	5.3016
	SolvBERT-QM-logS	1.1233	2.6173	2.1327
	GROVER-logS	0.0066	3.6388	0.6401
Ethanol	Measured	1.4266	4.8422	3.6682
	SolvBERT-QM-logS	1.9220	4.0771	3.2472
	GROVER-logS	0.0026	0.6187	0.5715

SolvBERT and GROVER were compared to the experimentally measured value for each combination.

The results show that out of the total 21 out-of-sample solute-solvent combinations, SolvBERT gives 11 predictions with relative errors less than 25% and 8 predictions with relative

errors between 25% and 75%. In contrast, GROVER gives 0 predictions with relative errors less than 25%, but 16 predictions with relative errors higher than 75%. Thus, our SolvBERT model significantly outperforms GROVER in predicting out-of-sample solubility data.



Table 6 Experimentally measured, SolvBERT-predicted, and GROVER-predicted solubility (g/100 g) with in-sample solutes and out-of-sample solvents. Experiments were performed at room temperature and 101.325 kPa

Out-of-sample solvent		In-sample solute		
		1,4-Naphthoquinone	Anthracene	4-Chlorophthalic anhydride
Propanol	Measured	2.3501	0.1924	3.7477
	SolvBERT-QM-logS	1.9579	0.0785	3.2751
	GROVER-logS	0.1417	0.2818	0.0427
Dichloromethane	Measured	4.0199	1.3657	5.0050
	SolvBERT-QM-logS	4.6786	3.2678	5.1182
	GROVER-logS	0.3627	0.0672	0.4066

Table 7 Experimentally measured, SolvBERT-predicted, and GROVER-predicted solubility (g/100 g) with out-of-sample solutes and out-of-sample solvents. Experiments were performed at room temperature and 101.325 kPa

Out-of-sample solvent		Out-of-sample solute		
		O-Methyl-N-nitrosoourea	3-Methyl-2-nitrobenzoic acid	2-Amino-5-chloro-3-methylbenzoic acid
Methanol	Measured	2.6491	2.5303	3.2882
	SolvBERT-QM-logS	2.8350	3.8242	4.2751
	GROVER-logS	0.0014	0.4522	0.5031
Propanol	Measured	2.0917	0.6267	1.4661
	SolvBERT-QM-logS	4.4350	0.7406	1.4601
	GROVER-logS	0.0012	0.3509	0.4434
Ethyl acetate	Measured	5.7051	3.5050	2.4918
	SolvBERT-QM-logS	1.8873	2.7925	2.6461
	GROVER-logS	0.0026	1.0075	0.2499

Discussion

One feature that distinguishes SolvBERT from graph-based models^{5,10,44} and a previously developed NLP model for solvation free energy or solubility prediction is that SolvBERT reads SMILES representation of solute–solvent pairs instead of reading solutes and solvents separately. Previously developed model architectures, such as *chemprop* and *Delfos*, use separate series of feature extraction layers for solutes and solvents, and then concatenate the extracted features into fully connected layers. In contrast, SolvBERT, as a BERT-derived model, treats the solute and solvent as a combination and maps a large number of such combinations into a chemical space, as is visualized by TMAP in Fig. 5. Such an approach not only enables a rapid search of nearest neighbors (*i.e.*, similar solute–solvent pairs), but also enables a more flexible representation of molecular complexes. Similar flexible representations have been seen in the classification²⁷ and yields prediction²⁸ of chemical reactions in the study of Schwaller *et al.* In their BERT-based model, no split of reactants, reagents, catalysts, and solvent is required, and these components of the reaction are mapped as a whole into a chemical space.

Another unique feature of SolvBERT is its unsupervised pre-training phase, which does not require any property data of the molecular complex. This feature has two benefits. First, larger and cheaper databases, such as CombiSolv-QM, can be used to pre-train the model without considering the potential impact of

different data fidelity (*i.e.*, computational vs. experimental) or difference property types (*i.e.*, ΔG for the CombiSolv-QM dataset and $\log S$ for the solubility dataset), since no target data are required in unsupervised learning. In addition, the model being pre-trained will be familiar with the molecular structure of the system and can be fine-tuned to predict multiple properties of the system (*i.e.*, solvation free energy and solubility for the solvation system), which requires a much smaller dataset than training a model from the beginning. This unique feature is particularly useful in cases where training datasets of different properties are significantly different in size or have little overlap in their chemical space, making it difficult for traditional multi-task deep learning to merge all these datasets into a single database.

We conclude this study by noting the recently published GNN-Transformer hybrid model GROVER,³⁹ which emerged as a new state-of-the-art model for molecular property prediction. Similar to our SolvBERT, GROVER includes a self-supervised pre-training phase and a down-stream supervised fine-tuning phase.³⁹ Although GROVER was comparable to SolvBERT in predictions from the CombiSolv-Exp-8780 and solubility datasets, it performed significantly worse in the out-of-sample predictions from our experimentally-measured dataset. One possible reason for this divergence between the two models in prediction of out-of-sample data is the nature of pre-training datasets. The GROVER model was pre-trained on 11 million (M) unlabeled molecules³⁹ selected from ZINC15 and ChemBL,



while our SolvBERT model was pre-trained on the CombiSolv-QM dataset that contains ~1 M combinations of solvents and solutes. In addition, the impressive clustering ability of solute-solvent combinations during the pre-training phase, which has been demonstrated in this study using TMAP visualization, may also help SolvBERT to better understand the solvation system. After all, we have to admit that since the model architecture of GROVER is significantly larger³⁹ than that of SolvBERT (48.8 M vs. 7.6 M), it is difficult to retrain GROVER on the CombiSolv-QM dataset with our current computational resources to give an absolutely fair comparison. Since SolvBERT takes only 12 hours to fully pre-train and fine-tune the model using only 1 Nvidia RTX 3060 GPU, while the GROVER-base requires 2.5 days using 250 Nvidia V100 GPUs,³⁹ SolvBERT can be considered as a more efficient model for predicting solvation-related properties.

Conclusion

An NLP-based deep learning model, SolvBERT, was developed to predict solvation free energy and solubility. Unlike graph-based models that read solutes and solvents separately, SolvBERT reads solute-solvent pairs through a combined SMILES representation. The model was pre-trained in an unsupervised learning manner, using a computational solvation free energy database containing 1 million combinations of solutes and solvents. The model was then fine-tuned with a regression layer on either the experimental solvation free energy database or the solubility database, depending on the type of regression task. The results showed that pre-training SolvBERT with a large computational solvation free energy database was beneficial for predicting the experimental solvation free energy, especially when the experimental fine-tuning dataset was small in size. Moreover, the performance of SolvBERT was comparable to that of the state-of-the-art graph-based model, DMPNN, and a recently-developed graph-Transformer hybrid model, GROVER. In addition, TMAP visualization of solute-solvent combination clustering showed the benefits of the unsupervised learning phase of SolvBERT in facilitating the clustering of solvent combinations with similar solvation properties. Finally, an out-of-sample solubility dataset was experimentally measured, and SolvBERT was found to have better prediction performance than GROVER on this dataset.

We also summarized two unique features of SolvBERT compared to graph-based models and non-BERT NLP models. SolvBERT is more flexible in representing molecular complexes, allowing not only the search for similar complexes by mapping in chemical space, but also the extension of molecular complexes beyond two components. In addition, the pre-training phase of SolvBERT does not require any attribute data, suggesting that it is possible to use the BERT-based model to predict multiple properties regardless of the differences in the size, fidelity, or attributes of training datasets. We recommend that researchers apply SolvBERT to at least three situations in future studies: (1) predicting different properties of chemical reactions, including the selectivity, conversion rates, and environmental impacts; (2) predicting different biological

activities of molecules; (3) predicting the properties of molecular complexes containing more than two components.

Code availability

The code supporting the finding of this study has been deposited at figshare⁴³ and GitHub (<https://github.com/su-group/SolvBERT>). All codes required for SolvBERT and TMAP, as well as repeating data pre-processing, is included in the “solv-bert” folder. The folder also contains a detailed SolvBERT instruction manual, and the code for TMAP is placed in the “tmapfiles” folder, where the “tmapfiles/TMAP” folder has high-resolution images.

The open source version we use is as follows: torch 1.11.0 + cu113, python 3.7.13, rxnfp 0.0.7, tokenizers 0.7.0, wandb 0.12.15, tmap1.0.6, fearun 0.3.20, mhfp1.9.2, sklearn 0.23.1, matplotlib 3.2.2, Pandas 1.3.4.

Data availability

The authors declare that the main data supporting the finding of this study are available within the article. All the supporting data have been deposited at figshare⁴³ and GitHub (<https://github.com/su-group/SolvBERT>). The supporting data are in the “solv-bert/data” folder, while the data used for training are placed in the “solv-bert/data/training_files” folder.

Conflicts of interest

There are no conflicts of interest to declare.

Acknowledgements

We gratefully acknowledge Zhejiang Province Science and Technology Plan Project (No. 2019- ZJ-JS-03), National Natural Science Foundation of China (No. 22108252), and Zhejiang Province Science and Technology Plan Project (No. 2022C01179) for financial support.

References

- 1 C. W. Coley, W. H. Green and K. F. Jensen, Machine learning in computer-aided synthesis planning, *Acc. Chem. Res.*, 2018, **51**(5), 1281–1289.
- 2 F. Strieth-Kalthoff, F. Sandfort, M. H. S. Segler and F. Glorius, Machine learning the ropes: principles, applications and directions in synthetic chemistry, *Chem. Soc. Rev.*, 2020, **49**(17), 6154–6168.
- 3 R. Gómez-Bombarelli, J. N. Wei, D. Duvenaud, J. M. Hernández-Lobato, B. Sánchez-Lengeling, D. Sheberla, J. Aguilera-Iparraguirre, T. D. Hirzel, R. P. Adams and A. Aspuru-Guzik, Automatic chemical design using a data-driven continuous representation of molecules, *ACS Cen. Sci.*, 2018, **4**(2), 268–276.
- 4 B. Sanchez-Lengeling and A. Aspuru-Guzik, Inverse molecular design using machine learning: generative



- models for matter engineering, *Science*, 2018, **361**(6400), 360–365.
- 5 D. K. Duvenaud; D. Maclaurin; J. Iparraguirre; R. Bombarell; T. Hirzel; A. Aspuru-Guzik and R. P. Adams, Convolutional networks on graphs for learning molecular fingerprints, in *Advances in Neural Information Processing Systems*, 2015, vol. 28, pp. 2224–2232.
- 6 T. Lei; W. Jin; R. Barzilay and T. Jaakkola, Deriving neural architectures from sequence and graph kernels, in *Proceedings of the 34th International Conference on Machine Learning*, ed. P. Doina and T. Yee Whye, PMLR: Proceedings of Machine Learning Research, 2017, vol. 70, pp. 2024–2033.
- 7 J. Gilmer; S. S. Schoenholz; P. F. Riley; O. Vinyals and G. E. Dahl, Neural message passing for quantum chemistry, in *Proceedings of the 34th International Conference on Machine Learning*, ed. P. Doina and T. Yee Whye, PMLR: Proceedings of Machine Learning Research, 2017, vol. 70, pp. 1263–1272.
- 8 H. Dai; B. Dai and L. Song, Discriminative embeddings of latent variable models for structured data, in *Proceedings of The 33rd International Conference on Machine Learning*, ed. B. Maria Florina and Q. W. Kilian, PMLR: Proceedings of Machine Learning Research, 2016, vol. 48, pp. 2702–2711.
- 9 C. W. Coley, R. Barzilay, W. H. Green, T. S. Jaakkola and K. F. Jensen, Convolutional embedding of attributed molecular graphs for physical property prediction, *J. Chem. Inf. Model.*, 2017, **57**(8), 1757–1772.
- 10 W.-L. Chiang; X. Liu; S. Si; Y. Li; S. Bengio and C.-J. Hsieh, Cluster-GCN, in *Proceedings of the 25th ACM SIGKDD International Conference on Knowledge Discovery & Data Mining*, 2019, pp. 257–266.
- 11 S. Ryu, Y. Kwon and W. Y. Kim, A Bayesian graph convolutional network for reliable prediction of molecular properties with uncertainty quantification, *Chem. Sci.*, 2019, **10**(36), 8438–8446.
- 12 L. Hirschfeld, K. Swanson, K. Yang, R. Barzilay and C. W. Coley, Uncertainty quantification using neural networks for molecular property prediction, *J. Chem. Inf. Model.*, 2020, **60**(8), 3770–3780.
- 13 A. P. Soleimany, A. Amini, S. Goldman, D. Rus, S. N. Bhatia and C. W. Coley, Evidential deep learning for guided molecular property prediction and discovery, *ACS Cent. Sci.*, 2021, **7**(8), 1356–1367.
- 14 A. Vaswani; N. Shazeer; N. Parmar; J. Uszkoreit; L. Jones; A. N. Gomez; Ł. Kaiser and I. Polosukhin, Attention is all you need, in *Advances in Neural Information Processing Systems*, 2017, vol. 30, pp. 5998–6008.
- 15 P. Schwaller, T. Laino, T. Gaudin, P. Bolgar, C. A. Hunter, C. Bekas and A. A. Lee, Molecular transformer: a model for uncertainty-calibrated chemical reaction prediction, *ACS Cent. Sci.*, 2019, **5**(9), 1572–1583.
- 16 G. Pesciullesi, P. Schwaller, T. Laino and J.-L. Reymond, Transfer learning enables the molecular transformer to predict regio- and stereoselective reactions on carbohydrates, *Nat. Commun.*, 2020, **11**(1), 4874.
- 17 Y. Zhang, L. Wang, X. Wang, C. Zhang, J. Ge, J. Tang, A. Su and H. Duan, Data augmentation and transfer learning strategies for reaction prediction in low chemical data regimes, *Org. Chem. Front.*, 2021, **8**(7), 1415–1423.
- 18 P. Schwaller, R. Petraglia, V. Zullo, V. H. Nair, R. A. Haeuselmann, R. Pisoni, C. Bekas, A. Iuliano and T. Laino, Predicting retrosynthetic pathways using transformer-based models and a hyper-graph exploration strategy, *Chem. Sci.*, 2020, **11**(12), 3316–3325.
- 19 I. V. Tetko, P. Karpov, R. Van Deursen and G. Godin, State-of-the-art augmented NLP transformer models for direct and single-step retrosynthesis, *Nat. Commun.*, 2020, **11**(1), 5575.
- 20 S. Zheng, J. Rao, Z. Zhang, J. Xu and Y. Yang, Predicting retrosynthetic reactions using self-corrected transformer neural networks, *J. Chem. Inf. Model.*, 2020, **60**(1), 47–55.
- 21 A. Su, X. Wang, L. Wang, C. Zhang, Y. Wu, X. Wu, Q. Zhao and H. Duan, Reproducing the invention of a named reaction: zero-shot prediction of unseen chemical reactions, *Phys. Chem. Chem. Phys.*, 2022, **24**(17), 10280–10291.
- 22 J. Xu, Y. Zhang, J. Han, A. Su, H. Qiao, C. Zhang, J. Tang, X. Shen, B. Sun, W. Yu, S. Zhai, X. Wang, Y. Wu, W. Su and H. Duan, Providing direction for mechanistic inferences in radical cascade cyclization using a transformer model, *Org. Chem. Front.*, 2022, **9**(9), 2498–2508.
- 23 P. Schwaller, B. Hoover, J.-L. Reymond, H. Strobelt and T. Laino, Extraction of organic chemistry grammar from unsupervised learning of chemical reactions, *Sci. Adv.*, 2021, **7**(15), eabe4166.
- 24 A. C. Vaucher, F. Zipoli, J. Geluykens, V. H. Nair, P. Schwaller and T. Laino, Automated extraction of chemical synthesis actions from experimental procedures, *Nat. Commun.*, 2020, **11**(1), 3601.
- 25 A. C. Vaucher, P. Schwaller, J. Geluykens, V. H. Nair, A. Iuliano and T. Laino, Inferring experimental procedures from text-based representations of chemical reactions, *Nat. Commun.*, 2021, **12**(1), 2573.
- 26 J. Devlin, M.-W. Chang, K. Lee and K. J. A. Toutanova, Bert: Pre-training of deep bidirectional transformers for language understanding, 2018, arXiv preprint arXiv:1810.04805.
- 27 P. Schwaller, D. Probst, A. C. Vaucher, V. H. Nair, D. Kreutter, T. Laino and J.-L. Reymond, Mapping the space of chemical reactions using attention-based neural networks, *Nat. Mach. Intell.*, 2021, **3**(2), 144–152.
- 28 P. Schwaller, A. C. Vaucher, T. Laino and J.-L. Reymond, Prediction of chemical reaction yields using deep learning, *Mach. Learn. Sci. Technol.*, 2021, **2**(1), 015016.
- 29 K. Kwak, S. Park and M. D. Fayer, Dynamics around solutes and solute–solvent complexes in mixed solvents, *Proc. Natl. Acad. Sci., India*, 2007, **104**(36), 14221–14226.
- 30 K. Kwak, D. E. Rosenfeld, J. K. Chung and M. D. Fayer, Solute–solvent complex switching dynamics of chloroform between acetone and dimethylsulfoxide—two-dimensional ir chemical exchange spectroscopy, *J. Phys. Chem. B*, 2008, **112**(44), 13906–13915.



- 31 S. Boobier, D. R. J. Hose, A. J. Blacker and B. N. Nguyen, Machine learning with physicochemical relationships: solubility prediction in organic solvents and water, *Nat. Commun.*, 2020, **11**(1), 5753.
- 32 G. Xiong, Z. Wu, J. Yi, L. Fu, Z. Yang, C. Hsieh, M. Yin, X. Zeng, C. Wu, A. Lu, X. Chen, T. Hou and D. Cao, ADMETlab 2.0: an integrated online platform for accurate and comprehensive predictions of ADMET properties, *Nucleic Acids Res.*, 2021, **49**(W1), W5–W14.
- 33 G. D. R. Matos, D. Y. Kyu, H. H. Loeffler, J. D. Chodera, M. R. Shirts and D. L. Mobley, Approaches for calculating solvation free energies and enthalpies demonstrated with an update of the FreeSolv database, *J. Chem. Eng. Data*, 2017, **62**(5), 1559–1569.
- 34 B. Guo; S. Song; J. Chacko and A. Ghalambor, CHAPTER 15 – flow assurance, in *Offshore Pipelines*, ed. B. Guo, S. Song, J. Chacko, and A. Ghalambor, Gulf Professional Publishing, Burlington, 2005, pp. 169–214.
- 35 F. Eckert and A. Klamt, Fast solvent screening via quantum chemistry: COSMO-RS approach, *AIChE J.*, 2002, **48**(2), 369–385.
- 36 I. T. Ho, M. Matysik, L. M. Herrera, J. Yang, R. J. Guderlei, M. Laussegger, B. Schrantz, R. Hammer, R. A. Miranda-Quintana and J. Smiatek, Combination of explainable machine learning and conceptual density functional theory: applications for the study of key solvation mechanisms, *Phys. Chem. Chem. Phys.*, 2022, **24**(46), 28314–28324.
- 37 W. Zhang, L. Deng, L. Zhang and D. Wu, A survey on negative transfer, *IEEE/CAA J. Automat. Sin.*, 2022, 305–329.
- 38 Z. Wang; Z. Dai; B. Póczos and J. Carbonell, Characterizing and avoiding negative transfer, in *IEEE/CVF Conference on Computer Vision and Pattern Recognition (CVPR)*, 15–20 June 2019, 2019, pp. 11285–11294.
- 39 Y. Rong; Y. Bian; T. Xu; W. Xie; Y. Wei; W. Huang and J. Huang, Self-supervised graph transformer on large-scale molecular data, in *Advances in Neural Information Processing Systems*, 2020, vol. 33, pp. 12559–12571.
- 40 H. Lim and Y. Jung, Delfos: deep learning model for prediction of solvation free energies in generic organic solvents, *Chem. Sci.*, 2019, **10**(36), 8306–8315.
- 41 S. Jaeger, S. Fulle and S. Turk, Mol2vec: unsupervised machine learning approach with chemical intuition, *J. Chem. Inf. Model.*, 2018, **58**(1), 27–35.
- 42 K. T. Butler, D. W. Davies, H. Cartwright, O. Isayev and A. Walsh, Machine learning for molecular and materials science, *Nature*, 2018, **559**(7715), 547–555.
- 43 S. Boobier, D. R. J. Hose, A. J. Blacker and B. N. Nguyen, Machine learning with physicochemical relationships: solubility prediction in organic solvents and water, *Nat. Commun.*, 2020, **11**(1), 5753.
- 44 F. H. Vermeire and W. H. Green, Transfer learning for solvation free energies: from quantum chemistry to experiments, *Chem. Eng. J.*, 2021, **418**, 129307.
- 45 A. V. Marenich; C. P. Kelly; J. D. Thompson; G. D. Hawkins; C. C. Chambers; D. J. Giesen; P. Winget; C. J. Cramer and D. G. Truhlar, *Minnesota Solvation Database (MNSOL) Version 2012*, 2020.
- 46 D. L. Mobley and J. P. Guthrie, FreeSolv: a database of experimental and calculated hydration free energies, with input files, *J. Comput.-Aided Mol. Des.*, 2014, **28**(7), 711–720.
- 47 E. Moine, R. Privat, B. Sirjean and J.-N. Jaubert, Estimation of solvation quantities from experimental thermodynamic data: development of the comprehensive compsol databank for pure and mixed solutes, *J. Phys. Chem. Ref. Data*, 2017, **46**(3), 033102.
- 48 L. M. Grubbs, M. Saifullah, N. E. De La Rosa, S. Ye, S. S. Achi, W. E. Acree and M. H. Abraham, Mathematical correlations for describing solute transfer into functionalized alkane solvents containing hydroxyl, ether, ester or ketone solvents, *Fluid Phase Equilib.*, 2010, **298**(1), 48–53.
- 49 X. C. Zhang, C. K. Wu, Z. J. Yang, Z. X. Wu, J. C. Yi, C. Y. Hsieh, T. J. Hou and D. S. Cao, MG-BERT: leveraging unsupervised atomic representation learning for molecular property prediction, *Briefings Bioinf.*, 2021, **22**(6), bbab152.
- 50 J. Devlin, M.-W. Chang, K. Lee and K. J. A. Toutanova, BERT: pre-training of deep bidirectional transformers for language understanding, 2019, arXiv:1810.04805.
- 51 K. Yang, K. Swanson, W. Jin, C. Coley, P. Eiden, H. Gao, A. Guzman-Perez, T. Hopper, B. Kelley, M. Mathea, A. Palmer, V. Settels, T. Jaakkola, K. Jensen and R. Barzilay, Analyzing learned molecular representations for property prediction, *J. Chem. Inf. Model.*, 2019, **59**(8), 3370–3388.
- 52 D. Probst and J.-L. Reymond, A probabilistic molecular fingerprint for big data settings, *J. Cheminf.*, 2018, **10**(1), 66.
- 53 T. Sterling and J. J. Irwin, ZINC 15 – Ligand discovery for everyone, *J. Chem. Inf. Model.*, 2015, **55**(11), 2324–2337.
- 54 A. P. Bento, A. Gaulton, A. Hersey, L. J. Bellis, J. Chambers, M. Davies, F. A. Krüger, Y. Light, L. Mak, S. McGlinchey, M. Nowotka, G. Papadatos, R. Santos and J. P. Overington, The ChEMBL bioactivity database: an update, *Nucleic Acids Res.*, 2014, **42**(D1), D1083–D1090.
- 55 D. Probst and J.-L. Reymond, Visualization of very large high-dimensional data sets as minimum spanning trees, *J. Cheminf.*, 2020, **12**(1), 12.
- 56 A. Andoni; I. P. Razenshteyn and N. S. Nosatzki, in *LSH Forest: Practical Algorithms Made Theoretical*, ACM-SIAM Symposium on Discrete Algorithms, 2017.
- 57 J. B. Kruskal, in *On the Shortest Spanning Subtree of a Graph and the Traveling Salesman Problem*, 1956.
- 58 D. Probst and J.-L. Reymond, FUN: a framework for interactive visualizations of large, high-dimensional datasets on the web, *Bioinformatics*, 2018, **34**(8), 1433–1435.
- 59 X. Ying, An overview of overfitting and its solutions, *J. Phys.: Conf. Ser.*, 2019, **1168**.

